QUANTUM SIMULATIONS
OF STRONGLY COUPLED QUARK–GLUON PLASMA

V. S. Filinov [a, 1], *Yu. B. Ivanov* [b, c],
M. Bonitz [d], *P. R. Levashov* [a], *V. E. Fortov* [a]

[a] Joint Institute for High Temperatures, Russian Academy of Sciences, Moscow

[b] GSI Helmholtzzentrum für Schwerionenforschung, Darmstadt, Germany

[c] Kurchatov Institute, Moscow

[d] Institute for Theoretical Physics and Astrophysics,
Christian Albrechts University, Kiel, Germany

A strongly coupled quark–gluon plasma (QGP) of heavy constituent quasiparticles is studied by a path-integral Monte Carlo method, which improves the corresponding classical simulations by extending them to the quantum regime. It is shown that this method is able to reproduce the lattice equation of state and also yields valuable insight into the internal structure of the QGP. The results indicate that the QGP reveals liquid-like rather than gas-like properties. At temperatures just above the critical one it was found that bound quark–antiquark states still survive. These states are bound by effective string-like forces. Quantum effects turned out to be of prime importance in these simulations.

PACS: 12.38.Mh

INTRODUCTION

Investigation of properties of the quark–gluon plasma (QGP) is one of the main challenges of strong-interaction physics, both theoretically and experimentally. Many features of this matter were experimentally discovered at the Relativistic Heavy Ion Collider (RHIC) at Brookhaven. The most striking result, obtained from analysis of these experimental data [1], is that the deconfined quark–gluon matter behaves as an almost perfect fluid rather than a perfect gas, as could be expected from the asymptotic freedom.

There are various approaches to studying QGP. Each approach has its advantages and disadvantages. The most fundamental way to compute properties of the strongly interacting matter is provided by the lattice QCD [2–4]. Interpretation of these very complicated computations requires application of various QCD motivated, albeit schematic, models simulating various aspects of the full theory. Moreover, such models are needed in cases when the lattice QCD fails, e.g., at large baryon chemical potentials and out of equilibrium.

A semiclassical approximation, based on a point-like quasiparticle picture, has been introduced in [5]. It is expected that the main features of non-Abelian plasmas can be understood in simple semiclassical terms without the difficulties inherent in a full quantum field theoretical analysis. Independently the same ideas were implemented in terms of molecular

---

[1] E-mail: vladimir_filinov@mail.ru

dynamics (MD) [6]. Recently this MD approach was further developed in a series of works [7, 8]. The MD allowed one to treat soft processes in the QGP which are not accessible by perturbative means.

A strongly correlated behavior of the QGP is expected to show up in long-ranged spatial correlations of quarks and gluons which, in fact, may give rise to liquid-like and, possibly, solid-like structures. This expectation is based on a very similar behavior observed in electrodynamic plasmas [7, 9]. This similarity was exploited to formulate a classical nonrelativistic model of a color Coulomb-interacting QGP [7] which was numerically analyzed by classical MD simulations. Quantum effects were either neglected or included phenomenologically via a short-range repulsive correction to the pair potential. Such a rough model may become a critical issue at high densities. For temperatures and densities of the QGP considered in [7], these effects are very important as the quasiparticle thermal wavelength is of order the average interparticle distance.

In this contribution we extend previous classical nonrelativistic simulations [7] based on a color Coulomb interaction to the quantum regime. We develop an approach based on path integral Monte Carlo (PIMC) simulations of the strongly coupled QGP which self-consistently takes into account the Fermi (Bose) statistics of quarks (gluons). Following an idea of Kelbg [10], quantum corrections to the pair potential are rigorously derived [11]. This method has been successfully applied to strongly coupled electrodynamic plasmas [12, 13]. Examples are partially ionized dense hydrogen plasmas, where liquid-like and crystalline behavior was observed [14, 15]. Moreover, also partial ionization effects and pressure ionization could be studied from first principles [16]. The same methods have also been applied to electron–hole plasmas in semiconductors [17, 18], including excitonic bound states, which have many similarities to the QGP due to smaller mass differences as compared to electron–ion plasmas.

First results of applications of the PIMC method to the nonideal QGP have already been briefly reported in [19].

1. BASICS OF THE MODEL

Our model is based on a resummation technique and lattice simulations for dressed quarks, antiquarks and gluons interacting via the color Coulomb potential. The assumptions of the model are similar to those of [7]:

I. All color quasiparticles are heavy; i.e., their mass (m) is higher than the mean kinetic energy per particle. For instance, at zero net-baryon density it amounts to $m > T$, where T is a temperature. Therefore, these particles move nonrelativistically. This assumption is based on the analysis of lattice data [20, 21].

II. Since the particles are nonrelativistic, interparticle interaction is dominated by a color-electric Coulomb potential, see Eq. (1). Magnetic effects are neglected as subleading ones.

III. Relying on the fact that the color representations are large, the color operators are substituted by their average values, i.e., by classical color vectors, the time evolution of which is described by Wong's dynamics [22].

The quality of these approximations and their limitations were discussed in [7]. Thus, this model requires the following quantities as an input:

1) the quasiparticle mass, m, and

2) the coupling constant g^2.

All the input quantities should be deduced from the lattice data or from an appropriate model simulating these data.

Thus, we consider a three-component QGP consisting of a number of dressed quarks (N_q), antiquarks ($N_{\bar{q}}$) and gluons (N_g) represented by quasiparticles. In thermal equilibrium the average values of these numbers can be found in the grand canonical ensemble defined by the temperature-dependent Hamiltonian, which can be written as $\hat{H} = \hat{K} + \hat{U}$. The kinetic and color Coulomb interaction energy of the quasiparticles are

$$\hat{K} = \sum_i \left[m_i(T, \mu_q) + \frac{\hat{p}_i^2}{2m_i(T, \mu_q)} \right], \quad \hat{U} = \frac{1}{2} \sum_{i,j} \frac{g^2(|r_i - r_j|, T, \mu_q) \langle Q_i | Q_j \rangle}{4\pi |r_i - r_j|}. \quad (1)$$

Here the Q_i denotes Wong's color variable (8-vector in the $SU(3)$ group), T is the temperature and μ_q is the quark chemical potential. In fact, the quasiparticle mass and the coupling constant, as deduced from the lattice data, are functions of T and, in general, μ_q. Moreover, g^2 is a function of distance r, which produces a linearly rising potential at large r [23].

The thermodynamic properties in the grand canonical ensemble with given temperature T, chemical potential μ_q and fixed volume V are fully described by the grand partition function

$$Z(\mu_q, \beta, V) = \sum_{N_q, N_{\bar{q}}, N_g} \frac{\exp\left(\mu_q(N_q - N_{\bar{q}})/T\right)}{N_q! N_{\bar{q}}! N_g!} \sum_\sigma \int_V dr\, dQ\, \rho(r, Q, \sigma; N_q, N_{\bar{q}}, N_g; \beta), \quad (2)$$

where $\rho(r, Q, \sigma; N_q, N_{\bar{q}}, N_g; \beta)$ denotes the diagonal matrix elements of the density operator $\hat{\rho} = \exp\left(-\beta\hat{H}\right)$, and $\beta = 1/T$. Here σ, r and Q denote the spin, spatial and color degrees of freedom of all quarks, antiquarks and gluons in the ensemble, respectively. Correspondingly, the σ summation and integration $dr\, dQ$ run over all individual degrees of freedom of the particles. Since the masses and the coupling constant depend on the temperature and chemical potential, special care should be taken to preserve thermodynamical consistency of this approach. In order to preserve the thermodynamical consistency, thermodynamic functions such as pressure, P, entropy, S, baryon number, N_B, and internal energy, E, should be calculated through respective derivatives of the logarithm of the partition function:

$$P = \frac{\partial(T \ln Z)}{\partial V}, \qquad S = \frac{\partial(T \ln Z)}{\partial T},$$
$$N_B = \frac{1}{3} \frac{\partial(T \ln Z)}{\partial \mu_q}, \quad E = -PV + TS + 3\mu_q N_B. \quad (3)$$

This is a conventional way of maintaining the thermodynamical consistency in approaches of the Ginzburg–Landau type as they are applied in high-energy physics.

The exact density matrix of interacting quantum systems can be constructed using a path integral approach [24, 25] based on the operator identity $e^{-\beta\hat{H}} = e^{-\Delta\beta\hat{H}} \cdot e^{-\Delta\beta\hat{H}} \cdots e^{-\Delta\beta\hat{H}}$, where the r.h.s. contains $n + 1$ identical factors with $\Delta\beta = \beta/(n + 1)$, which allows us to

rewrite[1] the integral in Eq. (2):

$$\sum_\sigma \int dr^{(0)} dQ^{(0)} \, \rho(q^{(0)}, Q^{(0)}, \sigma; N_q, N_{\bar{q}}, N_g; \beta) =$$

$$= \int dr^{(0)} dQ^{(0)} dr^{(1)} dQ^{(1)} \cdots dr^{(n)} dQ^{(n)} \, \rho^{(1)} \cdot \rho^{(2)} \cdots \rho^{(n)} \times$$

$$\times \sum_\sigma \sum_{P_q} \sum_{P_{\bar{q}}} \sum_{P_g} (-1)^{\kappa_{P_q} + \kappa_{P_{\bar{q}}}} \mathcal{S}(\sigma, \hat{P}_q \hat{P}_{\bar{q}} \hat{P}_g \sigma') \, \hat{P}_q \hat{P}_{\bar{q}} \hat{P}_g \rho^{(n+1)} \big|_{r^{(n+1)} = r^{(0)}, \sigma' = \sigma} =$$

$$= \int dQ^{(0)} dr^{(0)} dr^{(1)} \cdots dr^{(n)} \, \tilde{\rho}(r^{(0)}, r^{(1)}, \ldots, r^{(n)}; Q^{(0)}; N_q, N_{\bar{q}}, N_g; \beta). \quad (4)$$

The spin gives rise to the spin part of the density matrix ($\mathcal{S}$) with exchange effects accounted for by the permutation operators $\hat{P}_q$, $\hat{P}_{\bar{q}}$ and $\hat{P}_g$ acting on the quark, antiquark and gluon spatial $r^{(n+1)}$ and color $Q^{(n+1)}$ coordinates, as well as on the spin projections σ'. The sum runs over all permutations with parity κ_{P_q} and $\kappa_{P_{\bar{q}}}$. In Eq. (4) the index $l = 1, \ldots, n+1$ labels the off-diagonal density matrices $\rho^{(l)} \equiv \rho\left(r^{(l-1)}, Q^{(l-1)}; r^{(l)}, Q^{(l)}; \Delta\beta\right) \approx \langle r^{(l-1)} | e^{-\Delta\beta \hat{H}} | r^{(l)} \rangle \delta_\epsilon(Q^{(l-1)} - Q^{(l)})$, where $\delta_\epsilon(Q^{(l-1)} - Q^{(l)})$ is a delta function at $\epsilon \to 0$. Accordingly, each a particle is represented by a set of $n + 1$ coordinates («beads»), i.e., by $(n + 1)$ 3-dimensional vectors $\{r_a^{(0)}, \ldots, r_a^{(n)}\}$ and an 8-dimensional color vector $Q^{(0)}$ in the $SU(3)$ group, since all beads are characterized by the same color charge.

The main advantage of the decomposition (4) is that it allows us to use a semiclassical approximation for density matrices $\rho^{(l)}$, which is applicable due to smallness of artificially introduced factor $1/(n+1)$. This parameter makes the thermal wavelength $\Delta\lambda_a = \sqrt{2\pi\Delta\beta/m_a}$ of a bead of type a ($a = q, \bar{q}, g$), smaller than a characteristic scale of variation of the potential energy. In the high-temperature limit ρ^l can be approximated by a product of two-particle density matrices. Generalizing the electrodynamic plasma results [13] to the case of an additional bosonic species (i.e., gluons), we write

$$\tilde{\rho}(r^{(0)}, r^{(1)}, \ldots, r^{(n)}; Q^{(0)}; N_q, N_{\bar{q}}, N_g; \beta) =$$

$$= \sum_{s,k} \frac{C_{N_q}^s}{2^{N_q}} \frac{C_{N_{\bar{q}}}^k}{2^{N_{\bar{q}}}} \frac{\exp\{-\beta U(r, Q, \beta)\}}{\lambda_q^{3N_q} \lambda_{\bar{q}}^{3N_{\bar{q}}} \lambda_g^{3N_g}} =$$

$$= \text{per} \, ||\tilde{\phi}^{n,0}||_{\text{glue}} \det ||\tilde{\phi}^{n,0}||_s \det ||\tilde{\phi}^{n,0}||_k \prod_{l=1}^{n} \prod_{p=1}^{N} \phi_{pp}^l, \quad (5)$$

where $N = N_q + N_{\bar{q}} + N_g$, s and k are numbers of quarks and antiquarks, respectively, with the same spin projection, $\lambda_a = \sqrt{2\pi\beta/m_a}$ is a thermal wavelength of an a particle, $C_{N_a}^s = N_a! / [s!(N_a - s)!]$, the antisymmetrization and symmetrization are taken into account by the symbols «det» and «per» denoting the determinant and permanent, respectively. Functions $\phi_{pp}^l \equiv \exp\left[-\pi \left|\xi_p^{(l)}\right|^2\right]$ and matrix elements $\tilde{\phi}_{to}^{n,0} = \exp\left(-\pi \left|(r_t^{(0)} - r_o^{(0)}) + y_t^{(n)}\right|^2 / \Delta\lambda_a^2\right) \times$

---

[1]For the sake of notation convenience, we ascribe superscript $^{(0)}$ to the original variables.

$\times \delta_\epsilon(Q_t - Q_o)$, where t and o are particle's indexes, are expressed in terms of distances $(y_a^{(1)}, \ldots, y_a^{(n)})$ and dimensionless distances $(\xi_a^{(1)}, \ldots, \xi_a^{(n)})$ between neighboring beads of an a particle, defined as $r_a^{(l)} = r_a^{(0)} + y_a^{(l)}$, $l > 0$, and $y_a^{(l)} = \Delta\lambda_a \sum\limits_{k=1}^{l} \xi_a^{(k)}$. Notice that the $||\tilde{\phi}^{n,0}||$ matrix consists of three nonzero blocks related to quarks, $||\tilde{\phi}^{n,0}||_s$, antiquarks, $||\tilde{\phi}^{n,0}||_k$, and gluons, $||\tilde{\phi}^{n,0}||_{\mathrm{glue}}$. The density matrix (5) has been transformed to a form which does not contain an explicit sum over permutations. Let us stress that the determinants depend also on the color variables.

In Eq. (5) the total color interaction energy

$$U(r, Q, \beta) = \frac{1}{2(n+1)} \sum_{p \neq t} \sum_{l=1}^{n+1} \Phi^{pt}(|r_p^{(l-1)} - r_t^{(l-1)}|, |r_p^{(l)} - r_t^{(l)}|, Q_p, Q_t) \qquad (6)$$

is defined in terms of off-diagonal two-particle effective quantum potential Φ^{pt}, which is obtained by expanding the two-particle density matrix ρ_{pt} up to the first order in small parameter $1/(n+1)$:

$$
\begin{aligned}
\rho_{pt}(r, r', Q_p, Q_t, \Delta\beta) &\approx \rho_{pt}^0(r, r', Q_p, Q_t, \Delta\beta) - \\
&- \int_0^1 d\tau \int dr'' \frac{\Delta\beta g^2(|r''|, T, \mu_q)\langle Q_p|Q_t\rangle}{4\pi|r''|\Delta\lambda_{pt}^2 \sqrt{\tau(1-\tau)}} \exp\left(-\frac{\pi|r'-r''|^2}{\Delta\lambda_{pt}^2(1-\tau)}\right) \times \\
&\times \exp\left(-\frac{\pi|r''-r|^2}{\Delta\lambda_{pt}^2 \tau}\right) \approx \rho_{pt}^0 \exp\left[-\Delta\beta\Phi^{pt}(r, r', Q_p, Q_t)\right], \quad (7)
\end{aligned}
$$

where $r = r_p - r_t$, $r' = r'_p - r'_t$, $\Delta\lambda_{pt} = \sqrt{2\pi\Delta\beta/m_{pt}}$, $m_{pt} = m_p m_t/(m_p + m_t)$, and ρ_{pt}^0 is the two-particle density matrix of the ideal gas. The result for the diagonal color Kelbg potential can be written as

$$\Phi^{pt}(r, r, Q_p, Q_t) \approx \frac{g^2(T, \mu_q)\langle Q_p|Q_t\rangle}{4\pi\Delta\lambda_{pt}x_{pt}} \left\{1 - e^{-x_{pt}^2} + \sqrt{\pi}x_{pt}\left[1 - \mathrm{erf}(x_{pt})\right]\right\}, \qquad (8)$$

where $x_{pt} = |r_p - r_t|/\Delta\lambda_{pt}$. Here the function $g^2(T, \mu_q) = \overline{g^2(r'', T, \mu_q)}$, resulting from averaging of the initial $g^2(r'', T, \mu_q)$ over relevant distances of order $\Delta\lambda_{pt}$, plays the role of an effective coupling constant. Note that the color Kelbg potential approaches the color Coulomb potential at distances larger than $\Delta\lambda_{pt}$. What is of prime importance, the color Kelbg potential is finite at zero distance, thus removing in a natural way the classical divergences and making any artificial cut-offs obsolete. This potential is straightforward generalizations of the corresponding potentials of electrodynamic plasmas [26]. The off-diagonal elements of the effective interaction are approximated by the diagonal one by means of $\Phi^{pt}(r, r', Q_p, Q_t) \approx [\Phi^{pt}(r, r, Q_p, Q_t) + \Phi^{pt}(r', r', Q_p, Q_t)]/2$.

The described path-integral representation of the density matrix is exact in the limit $n \to \infty$. For any finite number n, the error of the above approximations for the whole product in the r.h.s. of Eq. (4) is of the order of $1/(n+1)$, whereas the error of each ρ^l is of the order of $1/(n+1)^2$, as was shown in [13].

The main contribution to the partition function comes from configurations in which the «size» of the cloud of beads of quasiparticles is of the order of their thermal wavelength λ_a, whereas characteristic distances between beads of each quasiparticle are of the order of $\Delta\lambda_a$.

2. TESTING THE METHOD WITHIN THE CANONICAL ENSEMBLE

To test the developed approach, we consider the QGP only at zero baryon density and further simplify the model by additional approximations, similarly to [7]:

IV. We replace the grand canonical ensemble by a canonical one. The thermodynamic properties in the canonical ensemble with given temperature T and fixed volume V are fully described by the density operator $\hat{\rho} = \mathrm{e}^{-\beta \hat{H}}$ with the partition function defined as follows:

$$Z(N_q, N_{\bar{q}}, N_g, V; \beta) = \frac{1}{N_q! N_{\bar{q}}! N_g!} \sum_{\sigma} \int\limits_V dr \, dQ \, \rho(r, Q, \sigma; \beta), \tag{9}$$

with $N_q = N_{\bar{q}}$ and hence $N_B = 0$. In order to preserve the thermodynamical consistency of this formulation, thermodynamic quantities should be calculated through respective derivatives of the logarithm of the partition function similarly to that in Eq. (3) with the exception that now N_a are independent variables.

V. Since the masses of quarks of different flavors extracted from lattice data are very similar, we do not distinguish between quark flavors. Moreover, we take the quark and gluon quasiparticle masses being equal because their values deduced from the lattice data [20, 21] are very close.

VI. Because of the equality of masses and approximate equality of number of degrees of freedom of quarks, antiquarks and gluons, we assume that these species are equally represented in the system: $N_q = N_{\bar{q}} = N_g$.

VII. For the sake of technical simplicity, the $SU(3)$ color group is replaced by $SU(2)$.

Thus, this simplified model requires an additional quantity as an input:

3) The density of quasiparticles $(N_q + N_{\bar{q}} + N_g)/V = n(T)$ as a function of the temperature.

Although this density is unknown from the QCD lattice calculations and we use it as a fit parameter, it is very important to partially overcome constraints of the above simplifications. First, it concerns the use of the $SU(2)$ color group, which first of all reduces the degeneracy factors of the quark and gluon states, as compared to the $SU(3)$ case, and thereby reduces pressure and all other thermodynamic quantities. A proper fit of the density allows us to remedy this deficiency of the normalization. Second, in fact we consider the system of single quark flavor; i.e., all quarks are identical, which also reduces the normalization of all thermodynamic quantities. The density fit cures the deficiency of this normalization, though the excessive anticorrelation of quarks remains.

Ideally the parameters of the model should be deduced from the QCD lattice data. However, presently this task is still quite ambiguous. Therefore, in the present simulations we take a possible (maybe, not the most reliable) set of parameters. Following [7, 21], the parametrization of the quasiparticle mass is taken in the form

$$\frac{m(T)}{T_c} = \frac{0.9}{(T/T_c - 1)} + 3.45 + \frac{0.4T}{T_c}, \tag{10}$$

where $T_c = 175$ MeV is the critical temperature. This parametrization fits the quark mass at two values of temperature obtained in the lattice calculations [20]. According to [20], the masses are quite large: $m_q/T \simeq 4$ and $m_g/T \simeq 3.5$. These are essentially larger than masses required for quasiparticle fits [27, 28] of the lattice thermodynamic properties of the QGP:

$m_q/T \simeq 1-2$ and $m_g/T \simeq 1.5-3$. Moreover, the pole quark mass $m_q/T \simeq 0.8$ was reported in recent work [29], as deduced from lattice calculations. Nevertheless, in spite of the fact that it obviously produces too high masses, we use the parametrization (10) in order to be compatible with the input of classical MD of [7]. The T-dependence of this mass is illustrated in Fig. 1, a.

The coupling constant used in the simulations is displayed in Fig. 1 as well. From the point of view of the QCD phenomenology [30], it is too high at low energies, i.e., at $T/T_c \simeq 1-2$. However, the high values of masses require such a large value of g^2, e.g., to be consistent with the HTL results for the quasiparticle masses. The large value of g^2 is also required to simulate larger values of Casimirs (defining the normalization of the color vectors) in the $SU(3)$ group as compared to the $SU(2)$ one used here. Moreover, such high g^2 are not inconsistent with the lattice data [31].

The density of quasiparticles, which is additionally required within the canonical-ensemble approach, was chosen on the condition of the best agreement of the calculated pressure with the corresponding lattice result, see Fig. 1, b. It was taken to be $n(T) = 0.24T^3$. At first glance, it is a very low density. For example, in the classical simulations of [7] it was taken as $n(T)/T^3 = 6.3$, which corresponds to the density of an ideal gas of *massless* quarks, antiquarks and gluons. Since the quasiparticles are very heavy in the present model (as well as in that of [7]), the latter density looks unrealistically high. Even in quasiparticle models [27, 28], where the masses are lower, the density turns out to be $n(T)/T^3 \approx 1.4$. Since Eq. (10) gives even larger masses than those in [27, 28] and in view of the adopted large coupling, the chosen value of $n(T)$ does not look too unrealistic. The T-dependence of $n(T)$ is presented in Fig. 1, a in terms of the mean interparticle distance $r_s(T)$ in units of $\sigma = 1/T_c = 1.1$ fm (Wigner–Seitz radius). Notice that the present choice of $n(T)$ corresponds to the relation $Tr_s(T) = 1$.

Thus, although the chosen set of parameters is still debatable, it is somehow self-consistent. In the future we are going to get rid of the $n(T)$ parameter, by applying the grand-canonical approach, and by using more moderate (and maybe realistic) sets of parameters.

Calculation of the equation of state (Fig. 1, b) was used to optimize the parameters of the model in order to proceed to predictions of other properties concerning the internal structure and in the future also nonequilibrium dynamics of the QGP. The plasma coupling
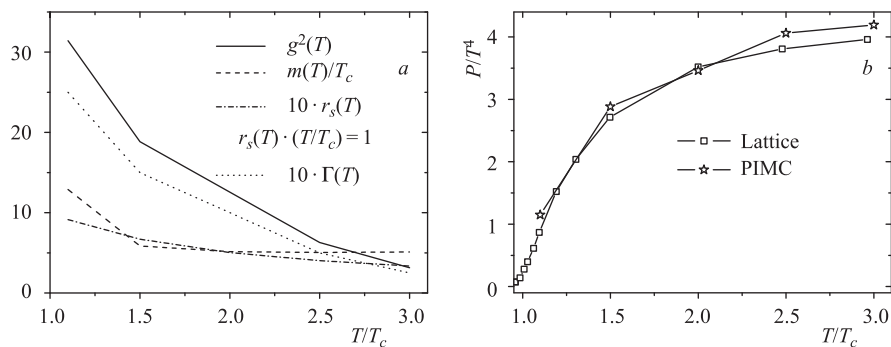
Fig. 1. a) Temperature dependence of the model input quantities and the plasma coupling parameter Γ. b) Equation of state (pressure versus temperature) of the QGP from PIMC simulations compared to lattice data of [2, 4]

parameter Γ, defined as a ratio of the average potential to average kinetic energy, is also presented in Fig. 1, a. It turns out to be of the order of unity, which indicates that the QGP is a strongly coupled Coulomb liquid rather than a gas. In the studied temperature range, $1 < T/T_c < 3$, the QGP is, in fact, quantum degenerate, since the degeneracy parameter $\chi_a = n_a \lambda_a^3$ varies from 0.1 to 2.

Let us now consider the spatial arrangement of the quasiparticles in the QGP by studying the pair distribution functions (PDFs) $g_{ab}(r)$. They give the probability density to find a pair of particles of types a and b at a certain distance r from each other and are defined as

$$g_{ab}(R_1 - R_2) = \frac{1}{Z N_q! N_{\bar{q}}! N_g!} \sum_\sigma \int dr\, dQ\, \delta(R_1 - r_1^a)\delta(R_2 - r_2^b)\rho(r, Q, \sigma; \beta). \qquad (11)$$

The PDFs depend only on the difference of cordinates because of the translational invariance of the system. In a noninteracting classical system, $g_{ab}(r) \equiv 1$, whereas interactions and quantum statistics result in a redistribution of the particles. Results for the PDFs at temperature $T/T_c = 3$ are shown in Fig. 2, a, b.

At large distances, $r/\sigma \geqslant 0.5$, all PDFs of identical particles (Fig. 2, a) coincide, approaching unity. At small distances, the gluon PDF increases monotonically when the distance goes to zero, while the PDF of quarks (and antiquarks) exhibits a broad maximum. In the present
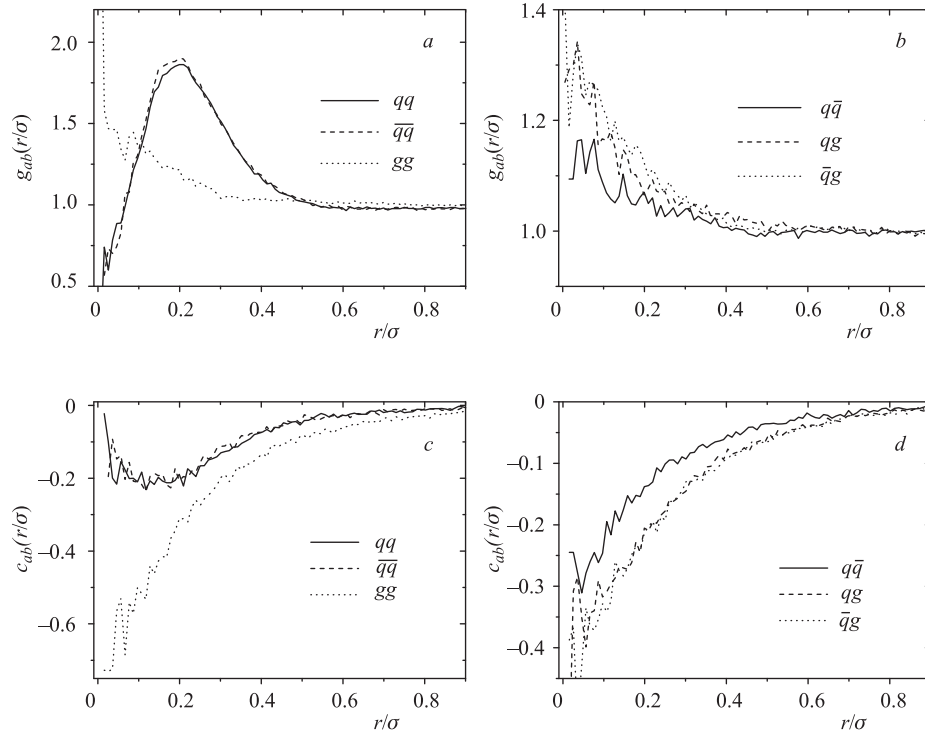
Fig. 2. Pair distribution functions (a, b) and color pair distribution functions (c, d) of identical (a, c) and different (b, d) quasiparticles at temperature $T/T_c = 3$, $\sigma = 1/T_c = 1.1$ fm

conditions, the thermal wavelength λ approximately equals 0.37σ; i.e., the difference starts to appear at distances of the order of λ. The enhanced population of low distance states of gluons is due to Bose statistics and the color-Coulomb attraction. In contrast, the depletion of the small distance range for quarks is a consequence of the Pauli principle. In an ideal Fermi gas $g(r)$ equals zero for particles with the same spin projections and colors, while for particles with different colors and/or opposite spins the PDF equals unity in the limit $r \rightarrow 0$. As a consequence, the spin and color averaged PDF approaches 0.5. Such a low-distance behavior is also observed in a nonideal dense astrophysical electron–ion plasma and in a nonideal electron–hole plasma in semiconductors [17,18]. The depletion of the probability of quasiparticles at small distances results in its enhancement at intermediate distances. This is the reason for the corresponding PDF maxima.

At small distances, $r \leqslant 0.3\sigma$, a strong increase is observed in all PDFs of particles of different type (Fig. 2, b), which resembles the behavior of the gluon–gluon PDF. This increase is a clear manifestation of an effective pair attraction of quarks and antiquarks as well as quarks (antiquarks) and gluons. This attraction suggests that the color vectors of nearest neighbors of any type are antiparallel. If this explanation is correct can be verified by means of *color pair distribution functions* (CPDF) defined as

$$c_{ab}(R_1 - R_2) = \frac{1}{ZN_q!N_{\bar{q}}!N_g!} \times$$
$$\times \sum_\sigma \int dr\, dQ\, \langle Q_1^a | Q_2^b \rangle \delta(R_1 - r_1^a) \delta(R_2 - r_2^b) \rho(r, Q, \sigma; \beta), \quad (12)$$

which are shown in Fig. 2, c, d. All CPDFs turn out to be negative at small distances, indicating antiparallel orientation of the color vectors of neighboring quasiparticles. The minimum of c_{qq} close to $r = 0.2\sigma$ corresponds to the maximum observed in g_{qq}. The deep minimum in the gluon CPDF at small distances results from the Bose statistics and complies with the high maximum of the gluon PDF g_{gg}.

Thus, at $T/T_c = 3$ we observe signs of a spatial ordering, cf. the peak of the quark PDF around $r/\sigma = 0.1-0.2$, which may be interpreted as emergence of liquid-like behavior of the QGP. The QGP lowers its total energy by minimizing the color Coulomb interaction energy via a spontaneous «antiferromagnetic» ordering of color vectors. This gives rise to a clustering of quarks, antiquarks and gluons.

Figure 3 presents PDFs of the identical particles for two temperatures $T = 1.1T_c$ and $T = 2T_c$ (panels a and c). These PDFs can be formed either by correlated scattering states or by bound states of quasiparticles, depending on the relative fractions of these states. In a strict sense, however, there is no clear subdivision into bound and free «components» due to the mutual overlap of the quasiparticle clouds. In addition, there exists no rigorous criterion for a bound state at high densities due to the strong effect of the surrounding plasma. Nevertheless, a rough estimate of the fraction of quasiparticle bound states can be obtained by the following reasonings. The product $r^2 g_{ab}(r)$ has the meaning of a probability to find a pair of quasiparticles at a distance r from each other. On the other hand, the corresponding quantum mechanical probability is the product of r^2 and the two-particle Slater sum

$$\Sigma_{ab} = 8\pi^{3/2}\lambda_{ab}^3 \sum_\alpha |\Psi_\alpha(r)|^2 \exp\left(-\beta E_\alpha\right) = \Sigma_{ab}^d + \Sigma_{ab}^c, \quad (13)$$
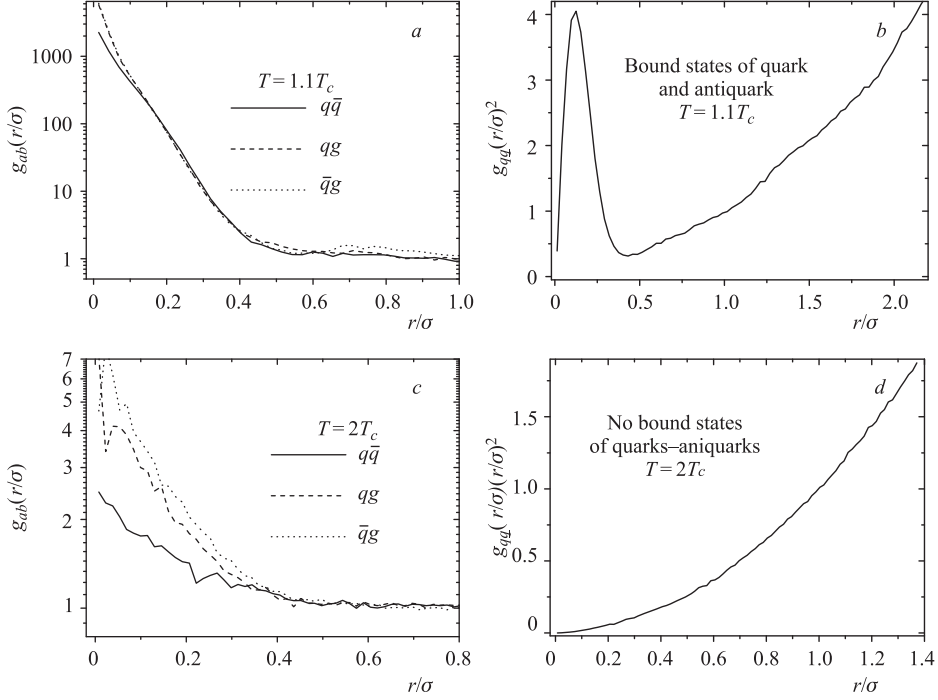
Fig. 3. Pair distribution functions at two different temperatures T (a, c) and quark–antiquark PDF multiplied by distance squared (b, d)

where E_α and $\Psi_\alpha(r)$ are the energy (without center-of-mass energy) and the wave function of a quasiparticle pair, respectively, and $\lambda_{ab} = \sqrt{2\pi\hbar^2\beta(m_a + m_b)/(m_a m_b)}$. Σ_{ab} is, in essence, the diagonal part of the corresponding density matrix. The summation runs over all states α of the discrete (Σ_{ab}^d) and continuous (Σ_{ab}^c) spectrum.

At temperatures smaller than the binding energy and distances smaller than or of the order of several bound state radii, the main contribution to the Slater sum comes from bound states. In the electromagnetic plasma it was found that the product $r^2\Sigma_{ab}^d$ is sharply peaked at distances around the Bohr radius in this case. Similarly, at low temperature, $r^2 g_{q\bar{q}}(r)$ forms a pronounced maximum near $r = 0.2$ fm, which can be interpreted as the radius of a bound $q\bar{q}$ pair. Thus, our calculations support the existence of bound states of medium-modified (massive) quarks and gluons at moderate temperatures, i.e., just above T_c, proposed in [33] and later in [34, 35] based on results from lattice QCD calculations of spectral functions [36, 37]. With the temperature rise these bound states dissolve much faster than it was assumed in [34, 35], which complies with the analysis of [38]. Indeed, at the temperature of $T = 2T_c$ the bound states completely disappear (Fig. 3, d).

Interesting observations can be done from the analysis of the potential of average force (PAF) defined as the logarithm of the related PDF, $U_{ab}(r, T) = -T \ln g_{ab}(r, T)$. This definition is motivated by the PDF virial expansion in terms of bare potential (like color Kelbg potential). Near the QGP phase transition the PAF is a linear function at distances smaller than the bound-state radius. This suggests that the bound states are bound by string-like forces. At larger distances the PAF can be very well approximated by an exponentially screened Coulomb potential (Yukawa-type potential) like that in the electromagnetic plasma.

CONCLUSION

Quantum Monte Carlo simulations based on the quasiparticle picture of the QGP are able to reproduce the lattice equation of state (even near the critical temperature) and also yield valuable insight into the internal structure of the QGP. Our results indicate that the QGP reveals liquid-like (rather than gas-like) properties even at the highest considered temperature of $3T_c$. At temperatures just above T_c we have found that bound quark–antiquark states still survive. These states are bound by effective string-like forces. Quantum effects turned out to be of prime importance in these simulations.

Our analysis is still too simplified and incomplete. It is still confined only to the case of zero baryon chemical potential. The input of the model also requires refinement. Work on these problems is in progress. We have also performed first simulations of dynamic properties of the QGP based on quantum Wigner dynamics. In particular, these allow us to deduce the viscosity of the QGP. However, the brief format of the present contribution does not allow us to report on the respective results.

REFERENCES

1. *Shuryak E.* // Prog. Part. Nucl. Phys. 2009. V. 62. P. 48.

2. *Bazavov A. et al.* arXiv:0903.4379 [hep-lat].

3. *Fodor Z., Katz S. D.* arXiv:0908.3341 [hep-ph].

4. *Csikor F. et al.* // JHEP. 2004. V. 0405. P. 046.

5. *Litim D. F., Manuel C.* // Phys. Rev. Lett. 1999. V. 82. P. 4981; Nucl. Phys. B. 1999. V. 562. P. 237; Phys. Rev. D. 2000. V. 61. P. 125004; Phys. Rep. 2002. V. 364. P. 451–539.

6. *Hofmann M. et al.* // Phys. Lett. B. 2000. V. 478. P. 161.

7. *Gelman B. A., Shuryak E. V., Zahed I.* // Phys. Rev. C. 2006. V. 74. P. 044908; 044909.

8. *Cho S., Zahed I.* // Phys. Rev. C. 2009. V. 79. P. 044911; V. 80. P. 014906; arXiv:0910.2666 [nucl-th]; arXiv:0910.1548 [nucl-th]; arXiv:0909.4725 [nucl-th]; *Dusling K., Zahed I.* // Nucl. Phys. A. 2010. V. 833. P. 172.

9. *Thoma M. H.* // IEEE Trans. Plasma Science. 2004. V. 32. P. 738.

10. *Kelbg G.* // Ann. Physik (Leipzig). 1962. V. 12. P. 219; 1963. V. 13. P. 354.

11. The idea to use a Kelbg-type effective potential also for quark matter was independently proposed in *Dusling K., Young C.* arXiv:0707.2068v2. However, their potentials are limited to weakly nonideal systems.

12. *Bonitz M. et al.* // J. Phys. A. 2003. V. 36. P. 5921; Phys. 2008. V. 15. P. 055704.

13. *Filinov V. S. et al.* // Plasma Phys. Control. Fusion. 2001. V. 43. P. 743.

14. *Filinov V. S., Bonitz M., Fortov V. E.* // JETP Lett. 2000. V. 72. P. 245.

15. *Bonitz M. et al.* // Phys. Rev. Lett. 2005. V. 95. P. 235006.

16. *Filinov V. S. et al.* // J. Phys. A. 2003. V. 36. P. 6069.

17. *Bonitz M. et al.* // J. Phys. A. 2006. V. 39. P. 4717.

18. *Filinov V. S. et al.* // Phys. Rev. E. 2007. V. 75. P. 036401.
19. *Filinov V. S. et al.* // Contrib. Plasma Phys. 2009. V. 49. P. 536.
20. *Petreczky P. et al.* // Nucl. Phys. Proc. Suppl. 2002. V. 106. P. 513.
21. *Liao J., Shuryak E. V.* // Phys. Rev. D. 2006. V. 73. P. 014509.
22. *Wong S. K.* // Nuovo Cim. A. 1970. V. 65. P. 689.
23. *Richardson J. L.* // Phys. Lett. B. 1979. V. 82. P. 272.
24. *Feynman R. P., Hibbs A. R.* Quantum Mechanics and Path Integrals. N. Y.; M.: McGraw-Hill, 1965.
25. *Zamalin V. M., Norman G. E., Filinov V. S.* The Monte Carlo Method in Statistical Thermodynamics. M.: Nauka, 1977 (in Russian).
26. *Filinov A. et al.* // Phys. Rev. E. 2004. V. 70. P. 046411.
27. *Peshier A., Kampfer B., Pavlenko O. P.* // Phys. Rev. D. 1996. V. 54. P. 2399.
28. *Ivanov Yu. B., Skokov V. V., Toneev V. D.* // Phys. Rev. D. 2005. V. 71. P. 014005.
29. *Karsch F., Kitazawa M.* arXiv:0906.3941v1 [hep-lat].
30. *Prosperi G. M., Raciti M., Simolo C.* // Prog. Part. Nucl. Phys. 2007. V. 58. P. 387.
31. *Kaczmarek O. et al.* // Phys. Rev. D. 2004. V. 70. P. 074505; Erratum // Phys. Rev. D. 2005. V. 72. P. 059903.
32. *Filinov A. V. et al.* Introduction to Computational Methods for Many-Body Physics / Eds.: M. Bonitz and D. Semkat. Princeton: Rinton Press, 2006.
33. *Yukalov V. I., Yukalova E. P.* // Physica A. 1997. V. 243. P. 382; Part. Nucl. 1997. V. 28. P. 89.
34. *Shuryak E. V., Zahed I.* // Phys. Rev. C. 2004. V. 70. P. 021901; 054507.
35. *Brown G. E., Gelman B. A., Rho M.* arXiv:nucl-th/0505037.
36. *Asakawa M., Hatsuda T., Nakahara Y.* // Prog. Part. Nucl. Phys. 2001. V. 46. P. 459; Nucl. Phys. A. 2003. V. 715. P. 863;
     Asakawa M., Hatsuda T. // Phys. Rev. Lett. 2004. V. 92. P. 012001.
37. *Datta S. et al.* // Phys. Rev. D. 2004. V. 69. P. 094507.
38. *Koch V., Majumder A., Randrup J.* // Phys. Rev. Lett. 2005. V. 95. P. 182301.